Single-Stage Visual Relationship Learning using Conditional Queries

Alakh Desai[1], Tz-Ying Wu[1], Subarna Tripathi[2], Nuno Vasconcelos[1]
[1]University of California San Diego, USA
[2]Intel Labs, USA

Abstract

Research in scene graph generation (SGG) usually considers two-stage models, that is, detecting a set of entities, followed by combining them and labelling all possible relationships. While showing promising results, the pipeline structure induces large parameter and computation overhead, and typically hinders end-to-end optimizations. To address this, recent research attempts to train single-stage models that are computationally efficient. With the advent of DETR[3], a set based detection model, one-stage models attempt to predict a set of subject-predicate-object triplets directly in a single shot. However, SGG is inherently a multi-task learning problem that requires modeling entity and predicate distributions simultaneously. In this paper, we propose Transformers with conditional queries for SGG, namely, **TraCQ** with a new formulation for SGG that avoids the multi-task learning problem and the combinatorial entity pair distribution. We employ a DETR-based encoder-decoder design and leverage conditional queries to significantly reduce the entity label space as well, which leads to 20% less parameters compared to state-of-the-art single-stage models. Experimental results show that TraCQ not only outperforms existing single-stage scene graph generation methods, it also beats many state-of-the-art two-stage methods on Visual Genome dataset, yet is capable of end-to-end training and faster inference.

1   Introduction

Scene graph generation (SGG) provides a structured representation of visual relations in a scene. A scene graph is a set of *subject-predicate-object* triplets, where subjects and objects are entity nodes in the graph and predicates are edges representing the relationship between pairs of entities. Due to its compact structure, SGG has been adopted as a foundational step for several high-level machine cognition tasks, including caption generation [48, 47, 29], visual question answering [13, 30], image retrieval [14, 38] and image generation [15, 22, 36]. However, SGG is far from a trivial problem, due to the complexity of detecting and pairing subject-object entities and inferring the predicate between each subject-object pair, requiring the model to excel at both entity and relationship detection. Hence, most research in the problem decomposes it into two separate sub-tasks, entity detection and predicate detection, which are modeled sequentially. This leverages success in object detection [7, 31] and leads to the predominance of two-stage networks in the literature [4, 52, 35, 34, 21, 43, 45, 25], where an object detector such as the faster-RCNN [31] solves the first sub-task, reducing the SGG modeling to the second stage that addresses the pairing of subject-object entities and classifying of predicate categories. The predicate detection part is typically achieved by ranking the $\mathcal{O}(N^2)$ triplet proposals generated by the exhaustive pairing of N entity predictions. While these models have shown promising results, the pipeline structure usually comes with significant parameter and computation overhead, which hinders end-to-end SGG optimization under memory constraints, and leads to sub-optimal solutions.

To enable end-to-end optimization, some recent works introduce one-stage models based on point-based detection [26] and transformer-based detectors [5, 33, 20]. Since SGG is inherently a multi-task learning problem, the main idea is to model the entity detection and predicate detection in parallel, which can be done in multiple ways. These models, however, face the problem of having to learn a joint feature space for two very different tasks. To circumvent the difficulty of this problem, they disentangle entity detection and predicate classification by training separate decoder branches for the two tasks. However, we hypothesize that this form of disentanglement is too strong for SGG, since capturing the interactions in a scene requires three kinds of features: f_e tuned for entity detection (object detection), f_p tuned for predicate classification, and f_i tuned for capturing the relationships between entities and their surroundings. While f_e can be learned well under a complete disentanglement of the two tasks, f_i is hard to capture without some amount of feature tuning for entity detection. In general, the task of predicate classification is what drives the learning of the interaction features. Therefore, f_p and f_i rely heavily on each other and benefit from some amount of coupled learning.

With this in mind, we propose Transformers with conditional queries (TraCQ), with a new formulation for scene graph generation. Instead of trying to learn f_e and f_i together in the entity detection branch, TraCQ learns f_p and f_i together in a predicate detection branch $\mathcal{H}$, which then conditions the learning of f_e by a separate entity refinement module $\mathcal{C}$. A weak coupling between predicate and entity detection is then ensured by forcing $\mathcal{H}$ to learn f_i through the prediction of loose estimates of subject and object bounding boxes. A major effect of this formulation is that the distribution that $\mathcal{H}$ learns is conditioned on the non-combinatorial predicate space, while typical SGG models disentangle the learning of f_p from (f_i, f_e) where the entity decoder is expected to learn a distribution based on the combinatorial $\mathcal{O}(\mathcal{E} \times \mathcal{E})$ space. Given that we have limited features and (f_i, f_p) are closely related, it is easier to learn from the non-combinatorial predicate space than the $\mathcal{O}(\mathcal{E} \times \mathcal{E})$ entity pair space. This reduction in distribution space implies that a simpler and smaller model can be used for SGG.

Overall, this paper makes the following contributions. First, we introduce a new formulation of the single-stage SGG task that avoids the multi-task learning problem and the combinatorial entity pair space. Second, we propose a novel architecture, Transformers with conditional queries (TraCQ), wherein conditional queries are leveraged to significantly reduce the inference time and the distribution space to learn, which leads to 20% less parameters compared to state-of-the-art single-stage models. Finally, we show that TraCQ achieves improved SGG performance than state-of-the-art methods on Visual Genome dataset, yet is capable of end-to-end training and faster inference.

2 Preliminaries

Transformers [37] are powerful models for sequence modeling, based on an encoder-decoder architecture. Both the encoder and the decoder modules stack multiple attention-based blocks, differing on the type of attention mechanisms employed. Encoding blocks perform self-attention across input tokens, while decoding blocks perform cross-attention between encoder output and predictions. The attention operation is defined over a set of queries $\mathbf{Q} \in \mathbb{R}^{n \times d_q}$, keys $\mathbf{K} \in \mathbb{R}^{n \times d_k}$ and values $\mathbf{V} \in \mathbb{R}^{n \times d_v}$, where $d_q = d_k$, according to

$$\text{Attention}(\mathbf{Q}, \mathbf{K}, \mathbf{V}) = \text{Softmax}\left(\frac{\mathbf{Q}\mathbf{K}^T}{\sqrt{d_k}}\right)\mathbf{V}. \tag{1}$$

Information from different representation subspaces is learned at different positions with resort to multihead attention based on different attention heads,

$$\text{MultiHead}(\mathbf{Q}, \mathbf{K}, \mathbf{V}) = \text{Concat}(\text{head}_1, \cdots, \text{head}_h)\mathbf{W}^O \quad \text{where } \mathbf{W}^O \in \mathbb{R}^{d_v \times h} \tag{2}$$

$$\text{head}_i = \text{Attention}(\mathbf{Q}\mathbf{W}_i^Q, \mathbf{K}\mathbf{W}_i^K, \mathbf{V}\mathbf{W}_i^V), \tag{3}$$

where $\{\mathbf{W}_i^Q, \mathbf{W}_i^K, \mathbf{W}_i^V\}$ are the parameters of the ith head. This is followed by a normalization layer [2] (LN) with residual connection in each block. We denote the entire module as the attention stack, $Attn_{stack}(\mathbf{Q}, \mathbf{K}, \mathbf{V})$, of queries $\mathbf{Q}$, keys $\mathbf{K}$ and values $\mathbf{V}$, moving forward.

DETR [3] is a Transformer-based object detector. A CNN backbone first generates a feature tensor $\mathbf{F}_b \in \mathbb{R}^{H \times W \times d}$ for an image $\mathcal{I}$. An encoder then learns context features $\mathbf{F}_v = Attn_{stack}(\mathbf{Q}_E, \mathbf{K}_E, \mathbf{V}_E) \in \mathbb{R}^{L \times d}$, where $L = H \times W$, $\mathbf{Q}_E = \mathbf{K}_E = \mathbf{V}_E = flatten(\mathbf{F}_b) + E_p$,

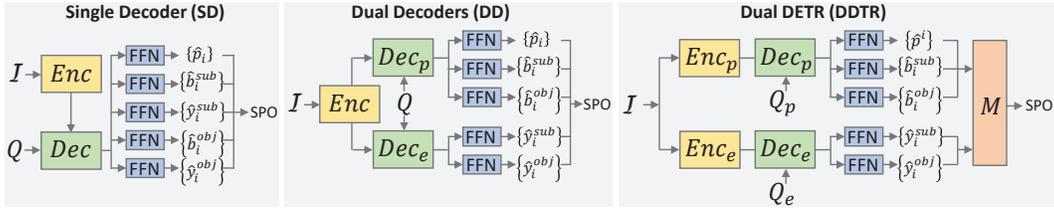Figure 1: **Baselines**. Enc, Dec, and M denote the encoder, decoder, and Hungarian matching respectively. $(\cdot)_p$ represents that the instance is for predicate detection, and $(\cdot)_e$ is for entity detection. SPO denotes triplets of <subject,predicate,object>.

and $E_p \in \mathbb{R}^{L \times d}$ is a fixed positional encoding. The decoder transforms a set of entity queries $\mathbf{Q}_{entity} \in \mathbb{R}^{N_e \times d_e}$ into entity representations

$$\mathbf{Z}_E = Attn_{stack}(\mathbf{Q}_{entity}, \mathbf{Q}_{entity}, \mathbf{F}_v) \in \mathcal{R}^{N_e \times d}. \tag{4}$$

Separate feed forward networks (FFNs) are finally used to predict each entity $\hat{e} = (\hat{b}, \hat{c})$, composed by class label $\hat{c}$ and a bounding box $\hat{b}$, from $\mathbf{Z}_E$.

DETR adopts a set prediction loss for entity detection, which performs bipartite matching between the ground truth set Y and the predicted set $\hat{Y}$ with the Hungarian matching algorithm [19], i.e.

$$\hat{\sigma} = \underset{\sigma \in \mathcal{G}_{N_e}}{\arg\min} \sum_{i=1}^{N_e} \mathcal{C}_{match}(\hat{e}_{\sigma(i)}, e_i), \tag{5}$$

where $\mathcal{G}_{N_e}$ denotes the set of permutations of N_e predicted entities, $e_i = (c_i, b_i) \in Y$, c, b indicate target class and box coordinates respectively, $\hat{e}_{\sigma(i)} \in \hat{Y}$,

$$\mathcal{C}_{match}(\hat{e}, e) = -\mathbb{1}_{\{c \neq \phi\}} \mathbf{p}_{\hat{e}}^c + \mathbb{1}_{\{c \neq \phi\}} \mathcal{L}_{box}(\hat{b}, b) \tag{6}$$

and $\mathbf{p}_{\hat{e}}^c$ is the logit for class c of entity $\hat{e}$. Note that Y is padded with background tokens ϕ. Finally, the set prediction loss is formulated as,

$$\mathcal{L}_{DETR} = \sum_{i=1}^{N_e} [\mathcal{L}_{cls}(\hat{c}_{\hat{\sigma}(i)}, c_i) + \mathbb{1}_{\{c_i \neq \phi\}} \mathcal{L}_{box}(\hat{b}_{\hat{\sigma}(i)}, b_i)], \tag{7}$$

where $\mathcal{L}_{cls}$ denotes the cross-entropy loss for label classification, $\mathcal{L}_{box}$ consists of L_1 and generalized IoU loss [32] for box coordinates regression.

In this work, we adopt a modified attention mechanism, namely Poll and Pool attention from PnP-DETR[39], which abstracts the image feature map into fine foreground object feature vectors and a small number of coarse background contextual feature vectors. We use PnP-DETR for faster convergence and computation efficiency.

3 Toward Single-Stage End-to-End Scene Graph Generation

3.1 Two-stage models

Given an image $\mathcal{I}$, scene graph generation produces a scene graph $\mathcal{G}$ to describe visual relations in a scene. $\mathcal{G}$ consists of a set of entity vertices $\mathcal{E}$, typically objects, and a set of directed edges $\mathcal{P}$ representing predicates, typically relationships between objects such as "to the left of." Each vertex in $\mathcal{E}$ is a tuple consisting of the bounding box b and the class label y of an entity instance, while each edge in $\mathcal{P}$ denotes the predicate label between a pair of entities. Each edge and its connected vertices form a relation tuple $< (b^{sub}, y^{sub}) - p - (b^{obj}, y^{obj}) >$, which is alternatively called *subject-predicate-object* (SPO) triplet, e.g. "a man in region b^{sub} - to the left of - a car in region b^{obj}." This is a complex task involving entity and predicate detection, which requires to model both entity and predicate distributions. Prior research [52, 6] usually models the problem as

$$Pr(\mathcal{G}|\mathcal{I}) = Pr(\mathcal{Y}, \mathcal{B}|\mathcal{I})Pr(\mathcal{P}|\mathcal{B}, \mathcal{Y}, \mathcal{I}), \tag{8}$$

Table 1: **Preliminary experiments.** The architectures of these baselines are presented in Figure 1.

Model	mean Recall (↑)			#params (↓) (M)	Inference time (↓) (sec)
	@20	@50	@100		
SD	5.7	6.2	6.3	41.7M	0.063
DD	6.5	6.9	7.0	51.1M	0.068
DDTR	9.2	11.8	13.0	82.9M	0.220

where $\mathcal{Y} = \{y_i\}_{i=1}^{|\mathcal{E}|}$ and $\mathcal{B} = \{b_i\}_{i=1}^{|\mathcal{E}|}$. A state-of-the-art object detector [7, 31] is then used to handle the first component, reducing the SGG problem to the second. While this two-stage formulation has produced good results, it leads to quite slow inference, since it requires an exhaustive search through the space of $\mathcal{O}(N^2)$. In addition, two-stage models usually have large parameter and computation overhead, which inhibits end-to-end SGG optimization, and makes the overall solution sub-optimal.

3.2 Learning scene graph generation with set predictions

With the advent of DETR [3], there has been a shift to single-stage end-to-end SGG learning, by adoption of a Transformer-based encoder-decoder architecture for SPO triplet set predictions. Several models have been proposed [5, 33, 20]. While efficient, these methods tend to have a weaker performance than two-stage models. We hypothesize that this is due to the entanglement between the feature spaces used to represent entities and predicates. This entanglement is unavoidable, since the detection of a predicate always requires some knowledge of the associated subject and object. However, a very strong entanglement is undesirable, because predicates and entities have very different distributions. Since the individual distributions of predicates and entities are long-tailed, the joint distribution of their pairs is extremely long-tailed. Hence, most pairs are very poorly represented in a highly entangled feature space.

We next test this hypothesis by performing some preliminary experiments on a set of baseline models of varying levels of disentanglement between the entity and predicate feature spaces.

Single decoder (SD) uses a pair of encoder and decoder modules, followed by five FFNs to decode each element $< (b^{sub}, y^{sub}) - p - (b^{obj}, y^{obj}) >$ of the SPO tuple. The encoder learns a context feature tensor from the input image $\mathcal{I}$, and the decoder takes these features and random queries $\mathcal{Q}$ to generate the FFN input. Since it generates the whole SPO triplet at once, this model learns a feature space where entities and predicates are highly entangled.

Dual decoders (DD) consists of a shared encoder and dual decoders for predicate and entity detection respectively, where the former decodes $< b^{sub} - p - b^{obj} >$ tuples and the latter decodes $< y^{sub} - y^{obj} >$ pairs. By feeding a common set of random queries $\mathcal{Q}$ to the two decoders, we ensure that no matching between the two output sets is needed. This is important to keep complexity competitive with that of SD. While introducing some additional cost, the use of two separate decoders encourages the disentanglement of the predicate and entity feature spaces. However, two architecture components still encourage entanglement: 1) the use of a common encoder and 2) the sharing of queries by the two decoders.

Dual DETRs (DDTR) avoids these problems by introducing separate DETR models, each with its own encoder, decoder and random queries, for detecting predicates and entities respectively. Similar to DD, one model decodes $< b^{sub} - p - b^{obj} >$, and the other $< y^{sub} - y^{obj} >$. Since each DETR has an individual set of random queries, a brute-forced matching between the two sets of outputs is needed to generate the detected graph. Assuming M predicates and N entity predictions, there are $M \times \mathbf{P}_2^N$ SPO tuples. Generating the cost matrix between the two sets is computationally expensive. However, this model also has the weakest entanglement between feature spaces.

In table 1, we compare the performance of these three baselines, in terms of mean Recall (see Section 5.1) on the Visual Genome (VG) [18] dataset. The number of parameters and the inference time are also provided. It is clear that disentangling predicate and entity representations is a good strategy for solving SGG. However, the computational cost of disjoint queries is quite high, including more parameters and lower inference speed. The question is whether the DD architecture can be improved to achieve performance closer to DDTR, while maintaining low parameter and computation overhead. To accomplish this, we next propose a model, TraCQ, based on the DD architecture. TraCQ
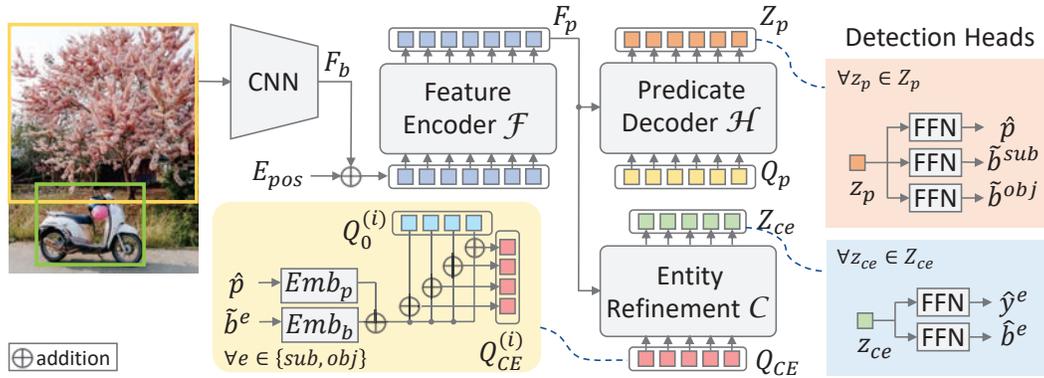
Figure 2: Model architecture of TraCQ.

reduces entanglement by replacing the shared queries of DD with conditional queries and leveraging decoupled training for predicates and entities.

4 Transformers with Conditional Queries

In this section, we introduce the proposed architecture, Transformers with conditional queries (TraCQ).

Architecture As shown in Figure 2, the TraCQ model employs the encoder-decoder Transformer design, composed of a feature extractor $\mathcal{F}$, a predicate decoder $\mathcal{H}$, and a conditional entity refinement decoder $\mathcal{C}$. The predicate decoder $\mathcal{H}$ predicts a set $\mathcal{S}_{pred}$ of $< b^{sub} - p - b^{obj} >$ tuples. The refinement decoder $\mathcal{C}$ predicts entity class labels and refines the bounding boxes detected by $\mathcal{H}$, to predict $< (b^{sub}, y^{sub}) - (b^{obj}, y^{obj}) >$ pairs. The idea is that, the use of $\mathcal{C}$ to refine the entity bounding boxes, frees $\mathcal{H}$ from solving this task with high accuracy. Hence, the feature space of $\mathcal{H}$ has to be less representative of entities, enhancing its disentanglement from the space of predicates. The details of each component are described below.

Feature Extractor The feature encoder $\mathcal{F}$ is a transformer encoder that takes a feature tensor $\mathbf{F}_b$ extracted from the image by the CNN backbone and a fixed positional encoding E_{Pos} and implements the self-attention stack to produce a feature tensor $\mathbf{F}_p$ that encodes the global image context. To ensure that $\mathbf{F}_p$ emphasizes attention on scene relations, $\mathcal{F}$ is trained jointly with $\mathcal{H}$ and then frozen for the training of $\mathcal{C}$. This results in features that are optimal for predicate detection. These features are richer than those for entity detection, since predicate detection involves an understanding of the constituent entities in order to detect the relationship between them and even captures the interplay between the entities in the scene which is difficult to learn if $\mathcal{F}$ was trained with $\mathcal{C}$.

The feature $\mathbf{F}_p$ is used as the $\mathbf{K}$ and $\mathbf{V}$ values for both decoders $\mathcal{H}$ and $\mathcal{C}$. This module, therefore, acts as the common encoder for both decoders.

Predicate Detection The predicate detection module $\mathcal{H}$ lies at the heart of TraCQ. This module comprises of a decoder which complements the encoder from $\mathcal{F}$. Similar to an entity detector, it transforms a set of predicate queries $\mathbf{Q}_p \in \mathcal{R}^{N_p \times d_p}$ into the predicate representations $\mathbf{Z}_P = Attn_{stack}(\mathbf{Q}_p, \mathbf{Q}_p, \mathbf{F}_p) \in \mathcal{R}^{N_p \times d}$. Hence, the composition of $\mathcal{F}$ and $\mathcal{H}$ is equivalent to that of DETR. However, $\mathbf{Z}_P$ is fed to three distinct multi-layer FFNs that learn to predict the bounding boxes $\tilde{b}^{sub}$ and $\tilde{b}^{obj}$ and the predicate class $\hat{p}$.

In this way, $\mathcal{H}$ learns to predict not only the predicate label but also a pair of bounding boxes for the subject and the object. This requires $\mathcal{H}$ to both learn to localize related entities and understand the relationship between them. However, predicting two bounding boxes along with the predicate label is far from trivial, due to the entanglement problems discussed above. To reduce entanglement, $\mathcal{H}$ learns to only roughly localize the subject and object, leaving the exact bounding box localization to $\mathcal{C}$. Since the key goal of the DETR-like combination of $\mathcal{F}$ and $\mathcal{H}$ is to predict predicate categories

accurately, it learns a visually rich feature space for the predicate distribution. Overall, $\mathcal{H}$ predicts a set $\mathcal{S}_{pred}$ of N_p 3-tuples $< \tilde{b}^{sub}, \hat{p}, \tilde{b}^{obj} >$, which is fed into the entity refinement module $\mathcal{C}$.

Conditioned Entity Refinement $\mathcal{C}$ While not accurate, the bounding boxes $\{\tilde{b}^{sub}, \tilde{b}^{obj}\}$ received from $\mathcal{H}$, provide an initial estimate of entity locations. The entity refinement model, $\mathcal{C}$, leverages these estimates to propose a set of N_{ce} refined bounding boxes $\{\hat{b}^{sub}, \hat{b}^{obj}\}$, conditioned on the predicate label estimate $\hat{p}$. This is implemented with a second decoder that shares the features $\mathbf{F}_p$ produced by the feature extractor $\mathcal{F}$ and a set of queries designed to induce the conditional operation.

For each bounding box estimate in $\mathcal{S}_{pred}$, $\mathcal{C}$ predicts N_{ce} refined entity bounding boxes. The queries used to generate these refinements are

$$Q_{ce}^{(i)} = Emb_b(\tilde{b}) + Emb_p(\hat{p}) + Q_0^{(i)} \text{ where } i \in \{1, 2, ..., N_{ce}\} , \tag{9}$$

$Emb_b(.)$ and $Emb_p(.)$ are two embeddings and $\mathbf{Q}_0$ is a DETR-like randomly generated set of N_{ce} queries, introduced to guarantee that the queries $Q_{ce}^{(i)}$ are distinct. From the conditional queries $\mathbf{Q}_{ce}$, $\mathcal{C}$ produces N_{ce} distinct corrections by computing representations $\mathbf{Z}_{ce} = Attn_{stack}(\mathbf{Q}_{ce}, \mathbf{Q}_{ce}, \mathbf{F}_p) \in \mathcal{R}^{N_{ce} \times d}$. It follows from (1)-(4) that the queries $\mathbf{Q}_{ce}$ bias the attention of $\mathcal{C}$ to the bounding boxes $\tilde{b}^{sub}$ and $\tilde{b}^{obj}$. This constraint encourages $\mathcal{C}$ to predict boxes in a substantially smaller region, thereby *limiting the box search space*. Furthermore, because attention is modulated by the predicted predicate label $\hat{p}$, this search is selective for boxes that comply with the former, which encourages agreement between entities and predicates, thus limiting the entity label search space.

For each bounding box in $\mathcal{S}_{pred}$, this process produces N_{ce} entity refinements, for a total of N_{ce}^2 5-tuples. k 5-tuples are chosen per predicate in $\mathcal{S}_{pred}$ to be part of the predicted scene graph $\mathcal{G}$, which contains $k \times N_p$ scene graph nodes.

Training TraCQ is trained with a set prediction loss for triplet detection that generalizes the entity detection set prediction loss of (7). Denote by $\hat{y}_{\mathcal{H}} = < \tilde{b}^{sub}, \hat{p}, \tilde{b}^{obj} >$ the prediction of $\mathcal{H}$, by $y_{\mathcal{H}} = < b^{sub}, p, b^{obj} >$ its groundtruth, by $\hat{y}_{\mathcal{C}} = < \hat{y}^e, \hat{b}^e >$ the entity correction of $\mathcal{C}$ and by $y_{\mathcal{C}} = < y^e, b^e >$ its groundtruth. TraCQ predicts N_p relationships, where N_p is larger than the number of relations in any given image. Similarly to DETR, this is handled by padding the ground truth set of relations with *no-relation* tokens ϕ. This circumvents a difficulty of single-stage models, which must account for the fact that relations of the types < valid subj - no rel - valid object> are different from those of the type < no subj - no rel - no object >, or other combinations. The predicate detection matching cost $\mathcal{C}_{match}(\hat{y}_{\mathcal{H}}, y_{\mathcal{H}})$ between a predicted and a ground truth triplet generalizes the matching cost function of (6), considering both the predicate class prediction and the similarity of predicted $\tilde{b}$ and ground truth b subject/object boxes, according to

$$\mathcal{C}_{match}(\hat{y}_{\mathcal{H}}, y_{\mathcal{H}}) = -\mathbb{1}_{\{p \neq \phi\}} \mathbf{p}_{y_{\mathcal{H}}}^p + \mathbb{1}_{\{p \neq \phi\}} [\mathcal{L}_{box}(\tilde{b}^{sub}, b^{sub}) + \mathcal{L}_{box}(\tilde{b}^{obj}, b^{obj})] \tag{10}$$

Similarly, the entity refinement matching cost $\mathcal{C}_{match}(\hat{y}_{\mathcal{C}}, y_{\mathcal{C}})$ uses both entity boxes and labels to calculate similarity, according to

$$\mathcal{C}_{match}(\hat{y}_{\mathcal{C}}, y_{\mathcal{C}}) = -\mathbb{1}_{\{y^e \neq \phi\}} \mathbf{p}_{y_{\mathcal{C}}}^{y^e} + \mathbb{1}_{\{y^e \neq \phi\}} \mathcal{L}_{box}(\hat{b}^e, b^e) \tag{11}$$

where the groundtruth entity e is either the subject (sub) or object (obj) entity of the corresponding prediction by $\mathcal{H}$. For both subject and object, the box alignment cost is

$$\mathcal{L}_{box}(\hat{b}, b) = \lambda_{gIoU} \mathcal{L}_{gIoU}(\hat{b}, b) + \lambda_{L_1} \mathcal{L}_{L_1}(\hat{b}, b)$$

Given the triplet cost matrix $\mathbf{C}_{match}$, the Hungarian algorithm [19] is executed for the bipartite matching and each ground truth triplet i is assigned to a predicted triplet $\hat{\sigma}(i)$. Let the $\hat{\sigma}_{\mathcal{H}}$ be the matching of $\mathcal{H}$ and $\hat{\sigma}_{\mathcal{C}}$ that of $\mathcal{C}$. Two losses are then defined as

$$\mathcal{L}_p = \sum_{i=1}^{N_p} \left[\lambda_{lbl} \mathcal{L}_{cls}(\hat{p}_j, p_i) + \mathbb{1}_{\{p_i \neq \phi\}} \{ \mathcal{L}_{box}(\tilde{b}_j^{sub}, b_i^{sub}) + \mathcal{L}_{box}(\tilde{b}_j^{obj}, b_i^{obj}) \} \right] \Big|_{j = \hat{\sigma}_{\mathcal{H}}(i)} \tag{12}$$

$$\mathcal{L}_e = \sum_{i=1}^{N_p} \mathbb{1}_{\{p_i \neq \phi\}} \left\{ \sum_{j=1}^{N_{ce}} [\lambda_{lbl} \mathcal{L}_{cls}(\hat{y}_k^e, y_j^e) + \mathbb{1}_{\{y_j^e \neq \phi\}} \mathcal{L}_{box}(\hat{b}_k^e, b_j^e)] \Big|_{k = \hat{\sigma}_{\mathcal{C}}(j)} \right\} \tag{13}$$

where $\mathcal{L}_{cls}$ is the cross-entropy loss. $\mathcal{F}$ and $\mathcal{H}$ are trained using $\mathcal{L}_p$, whereas $\mathcal{C}$ is trained with $\mathcal{L}_e$. This encourages the decoupling of feature spaces, encouraging the features of $\mathcal{F}$ and $\mathcal{H}$ to specialize in predicate prediction and those of $\mathcal{C}$ on predicate-conditioned entity detection.

Inference   The inference stage involves combining the outputs of entity refinement FFNs of $\mathcal{C}$ and the predicate detection FFNs of $\mathcal{H}$ to form final triplets. Due to the conditional structure of the decoder, the predicate detection outputs and the set of k entity refinement outputs have a one-to-one correspondence. Therefore, $k \times N_p$ SPO-tuples $< (b^{sub}, y^{sub}) - p - (b^{obj}, y^{obj}) >$ are automatically generated.

An SGG triplet score $s_{triplet}$ is computed per SPO-tuple with $s_{triplet} = s_{pred} s_{sub} s_{obj}$ where s_{sub} and s_{obj} are the scores of subject and object classification from $\mathcal{C}$, respectively, and s_{pred} is the predicate classification score from $\mathcal{H}$. Finally, the predictions are sorted by descending $s_{triplet}$ and the top $m < kN_p$ predictions selected as nodes of the predicted scene graph $\mathcal{G}$.

Comparison to previous approaches   When compared to two-stage SGG models, TraCQ replaces the model of (8) by

$$Pr(\mathcal{G}|\mathcal{I}) = \sum_{\hat{\mathcal{B}}} Pr(\mathcal{P}, \hat{\mathcal{B}}|\mathcal{I}) Pr(\mathcal{Y}, \mathcal{B}|\mathcal{P}, \hat{\mathcal{B}}, \mathcal{I}), \tag{14}$$

where $\hat{\mathcal{B}}$ is the set of bounding box estimates computed by $\mathcal{H}$ and the marginalization over $\hat{\mathcal{B}}$ is performed by the conditioning of the queries of $\mathcal{C}$ on the predictions of $\mathcal{H}$. Assume, for simplicity, that the labels $\mathcal{Y}, \mathcal{P}$ are independent of the bounding boxes $\mathcal{B}$. Then, (8) reduces to $Pr(\mathcal{G}|\mathcal{I}) = Pr(\mathcal{Y}|\mathcal{I}) Pr(\mathcal{B}|\mathcal{I}) Pr(\mathcal{P}|\mathcal{Y}, \mathcal{I})$ and its modeling complexity is dominated by the term $Pr(\mathcal{P}|\mathcal{Y}, \mathcal{I})$, which is a distribution conditioned the large combinatorial space of $O(\mathcal{E} \times \mathcal{E})$ entity pairs. On the other hand, (14) reduces to $Pr(\mathcal{G}|\mathcal{I}) = Pr(\mathcal{P}|\mathcal{I}) Pr(\mathcal{B}|\mathcal{I}) Pr(\mathcal{Y}|\mathcal{P}, \mathcal{I})$ and its complexity is determined by $Pr(\mathcal{Y}|\mathcal{P}, \mathcal{I})$, which is a distribution conditioned on the non-combinatorial space of predicates. Hence, TraCQ has an innate advantage over the two-stage models, the modeling of probabilities conditioned on much smaller spaces, which allows it to perform inference much more efficiently. Furthermore, the conditional queries $\mathbf{Q}_{ce}$ enforce something akin to ROI pooling, highly constraining the refinements made by $\mathcal{C}$. First, these are constrained to the region of the bounding boxes predicted by $\mathcal{H}$. Second, the queries are generated with the predicate label as well and therefore must learn only those entities that are consistent with this label.

When compared to single-stage models, TraCQ has the advantage of a feature representation where entities and predicates are less entangled, due to the training of the two decoders with different loss functions, and the use of decoder $\mathcal{C}$ to predict the entity labels and refine the bounding boxes predicted by $\mathcal{H}$. This places less stress on the training of $\mathcal{F}$ and $\mathcal{H}$ to produce high quality features for entity localization and encourages $\mathcal{C}$ to produce such features.

In other one-stage models, which predict combinations of entities and decouple just the predicate classification from entity classification, we observe that the features are not fully disentangled leading to drop in performance. The disentanglement induced by the predicate detection task reduces the feature representation space needed to detect the predicates and allows the use of a lightweight model to learn it.

5   Experiments

In this section, we present the results of TraCQ and ablates its components.

5.1   Settings

Dataset. Visual Genome (VG) [18] is a popular benchmark for SGG. While it is a large dataset containing 75k object categories and 37k predicate categories, both object and predicate distributions are highly long-tailed, where most of the categories only have few instances. Hence, a popular subset VG150 of VG is proposed by [43], which contains the most frequent 150 object classes and 50 predicate classes. We follow the setting of prior works, adopting VG150 in all the experiments.

Metrics. Since the annotations for SGG datasets are usually incomplete, early works in SGG are mostly evaluated with Recall@K (R@K). However, since SGG is a highly long-tailed problem, most recent research [4, 34] also present mean Recall@K (R@K), $K = \{20, 50, 100\}$ as the metric.

Table 2: Quantitative results of TraCQ in comparison with state-of-the-art methods on the VG dataset. TraCQ achieves new state-of-the-art results outperforming existing one-stage and two-stage models in most metrics, while reducing model complexity without the need for any extra features (e.g., glove vector, knowledge graph, etc.). Note that '-' indicates that the corresponding results are unavailable.

	Method	Extra Features	Backbone	mean-Recall (↑) @20	@50	@100	Recall (↑) @20	@50	@100	#params (↓) (M)
Two-Stage	MOTIFS[52]	✓	X-101FPN	4.2	5.7	6.6	21.4	27.2	30.5	240.7
	KERN[4]	✓	VGG16	-	6.4	7.3	22.3	27.1	-	405.2
	GPS-Net[25]	✓	VGG16	6.9	8.7	9.8	22.3	28.9	33.2	-
	BGNN[21]	✓	X-101FPN	7.5	10.7	13.6	23.3	31.0	34.6	341.9
	VCTree-TDE[34]	✓	X-101FPN	6.3	9.3	11.1	14.3	19.6	23.2	360.8
	IMP+[43]	✗	VGG16	2.9	3.8	4.8	14.6	20.7	24.5	203.8
	G-RCNN[45]	✗	VGG16	-	-	-	-	11.4	13.7	-
One Stage	FCSGG[26]	✗	HRNetW48-5S-FPN	2.7	3.6	4.2	16.1	21.3	25.1	87.1
	RelTR[5]	✗	ResNet-50	5.8	8.5	-	20.2	25.2	-	63.7
	Relationformer[33]	✗	ResNet-50	4.6	9.3	10.7	22.2	28.4	31.3	92.9
	TraCQ (ours)	✗	ResNet-50	**12.0**	**13.8**	**14.6**	19.7	28.3	**35.7**	**51.2**

5.2 Implementation details

The PnP-DETR[39] is set with sample ratio α of 0.33 and pool samples M of 60. We adopt ResNet-50 [10] with a 6-layer transformer encoder as the visual feature extractor $\mathcal{F}$. Both decoders $\mathcal{H}$ and $\mathcal{C}$ have a 6-layer transformer, with 8 and 4 attention heads respectively. The number of queries N_p is set to 200 and N_{ce} is set to 10 with $k = 5$. The FFNs for bounding box prediction have 3 linear layers with ReLU, while the FFNs for predicting object and relation labels have one linear layer.

We initialize the network with the parameters of PnP-DETR trained on VG for object detection, and adopt the default weight coefficients λ_{L_1}, λ_{GIoU} and λ_{lbl} from [39]. The network is optimized with AdamW [27] where the weight decay is 10^{-4}. The learning rates for training the backbone and the rest modules are 10^{-5} and 10^{-4} respectively. All experiments are conducted on 8 NVIDIA TITAN X GPUs, with total batch size of 32.

5.3 Comparisons to baselines

The baselines in Table 1 show the importance of disentanglement, where the performance increase from SD to DDTR. However, disjoint queries lead to large computational overhead due to the post-processing matching step and there is no way for further joint optimization. Learning from these baselines, TraCQ is a DD-type model leveraging decoupled training to disentangle the two distributions in representation learning while maintaining certain degree of dependence between the two tasks. As a result, TraCQ outperforms all these baselines with a large margin (2.8 point gain over DDTR in mR@20), while maintaining similar number of parameters as DD and achieving 1.5x faster inference than DDTR. This highlights that complete disentanglement is not possible, since the detection of a predicate always requires some knowledge of the associated subject and object.

5.4 Comparisons to prior methods

We compare scores of R@K, mR@K and number of parameters of TraCQ with several two-stage and one-stage models in Table 2. The usage of extra features such as semantic and statistic information by the model is indicated to distinguish those models from visual appearance based models. TraCQ beats all models in terms of mR@K while having 20% fewer parameters than [5], reportedly having the smallest model size. It also exhibits a much less drastic drop in the mean recall values when we go from 100 to 20 for mR@K. This shows that the model is more confident about it's predictions than others. In R@20 and R@50, TraCQ lags behind only those two-stage models, that are heavier and/or use extra features in their pipeline. TracQ is the first one-stage model that beats two-stage models in terms of performance with a much smaller model size.

5.5 Ablation studies

We perform the following ablations on TraCQ to understand the influence of each component.

Table 3: **Ablations on the orders** of entity detection and predicate detection.

Model	mean Recall (↑)		
	@20	@50	@100
Entity-first	11.2	12.3	12.7
Predicate-first (ours)	12.0	13.8	14.6

Table 4: **Ablation on the hyper-parameter k**. SGG is evaluated with mR@20 and R@20.

k	#Predictions (↓)	mR@20 (↑)	R@20 (↑)
1	**200**	8.9	18.4
5	1000	12.0	**19.7**
10	2000	**12.1**	**19.7**
15	3000	**12.1**	**19.7**

Table 5: **Ablation on bounding box refinements**.

Entity box prediction $\hat{b}^e$	mR@ 20 / 50 / 100
From $\mathcal{H}$ (no correction)	17.2 / 18.0 / 18.1
From $\mathcal{C}$ (ours)	16.9 / 18.6 / 19.2

Table 6: **Ablation on conditioned queries**.

Conditioned queries	mR@ 20 / 50 / 100
w/o $Emb_p(\hat{p})$	10.8 / 12.4 / 13.1
$\mathcal{Q}_{ce}$ (ours)	12.0 / 13.8 / 14.6

Ablations on the formulation   To validate the effectiveness of the proposed formulation, we also conduct the experiment of the entity-first variant. Different from TraCQ that predicts entity labels based on predicate predictions, this variant performs entity detection first and conditions predicate classification on it. We maintain similar setup as TraCQ on other components to ensure fair comparison. Table 3 shows that this variant underperforms the proposed formulation. This supports our idea of avoiding the combinatorial entity label space.

Ablations on the hyperparameter k   The hyperparameter k controls the number of candidate entity bounding boxes. We evaluate TraCQ with different values of k and present the mR@20 and R@20 in Table 4. We can see that the performance saturates quickly as the number of predictions (denoted as #Predictions) increases. Since the inference time is proportional to k, we pick $k = 5$.

Ablations on bounding box refinements   The entity refinement module, $\mathcal{C}$, performs entity detection using the global features and the conditioned queries of entity bounding boxes and predicates. To study how much box refinement was happening from H to $\mathcal{C}$, we directly take the predicted bounding box of subject and object, i.e. $\tilde{b}^{sub}$ and $\tilde{b}^{obj}$, from the predicate decoder $\mathcal{H}$ as the final prediction, but not correct the entity bounding boxes with $\mathcal{C}$. Since $\mathcal{H}$ does not produce class labels for subjects and objects, we evaluate the network in the task of Predicate Detection (PredDet), where ground-truth entity labels are given and the task is to predict $< b^{sub} - p - b^{obj} >$ tuples. Table 5 presents such results compared to TraCQ under the mR@K metric, which shows that the model performance drops when removing the entity refinement module.

Ablations on conditioned queries   We also ablate the impact of using the predicate labels $\hat{p}$ for generating the predicate conditioned queries $\mathcal{Q}_{ce}$ for $\mathcal{C}$. We retrain $\mathcal{C}$ conditioned only on the bounding boxes from $\mathcal{H}$, namely, removing $Emb_p(\hat{p})$ from (9). The bounding box conditioning cannot be removed, since that reduces $\mathcal{C}$ to a general entity set detection model. Table 6 presents the effect of removing the predicate conditioning for $\mathcal{C}$. The performance of the overall model drops by ~ 2 points at mR@20. This shows that the explicit condition forced onto $\mathcal{C}$ by the predicate conditioned queries does in fact reduce the searching space for inferring entity labels.

6   Related work

Scene graph generation (SGG) has long been studied in the literature due to its wide applicability [48, 47, 13, 14, 38, 15, 22, 36, 15, 22, 36]. Since SGG is a highly complex problem, pioneer works [18, 43, 52] leverage marginalization to decompose the problem into predicate classification, entity classification and entity localization. This formulation largely impacts the latter research. Most of the works follow the same pipeline structure which first detects a set of entity proposals with state-of-the-art object detectors [7, 31] and then classify all the pairs of entity proposals into a predicate class at the second stage. While object detection is considered as solved, most research focuses on learning a better mapping between entity pairs and predicate classes [54, 35, 4, 50, 24, 8, 23, 40, 42]. This can be achieved either by learning better representations for contextual reasoning [52, 21, 4, 41, 42, 46, 49, 17, 28], leveraging external knowledge [9, 51, 8, 50], or unbiased learning strategy [34, 25, 40, 1, 44, 6]. Among these, Relation Transformer Network[17] and Lu et

al [28] are pioneering works adopting Transformer encoder-decoder pair for learning SGG, while both of them rely on bounding box predictions from a CNN-based object detector. These research has provided insightful observations and promising results. However, the two-stage formulation has a fundamental problem, the searching space for relation detection is always $\mathcal{O}(N^2)$, which can retard the inference speed. In addition, building another computation module on top of a large object detector is inefficient in terms of parameters and computations, which prevents end-to-end optimizations for the SGG task.

To address this, [26, 5, 33, 20] propose one-stage models for SGG. [26] encodes objects as center points and relationships as vector fields. Although it is lightweight and fast, it has a significant performance gap compared to other two-stage methods. Others adopt DETR [3]-based architectures. RelTR[5] combines subject and object queries to decode the triplet predictions, while [33] produces a set of object tokens and a relation token, and decodes them respectively. [20] is a concurrent work that requires bipartite graph assembling similar to DDTR. While these works provide inspirational ideas and allows end-to-end optimizations, they still perform poor than two-stage methods. We hypothesize that the reason is because of the entangled feature space of entities and predicates. This paper focuses on a single-stage model with less entanglement between the two distributions.

Transformer-based Detection has become popular for many computer vision tasks recently. The pioneering work, DETR [3], introduces the set prediction with a Transformer encoder-decoder architecture, where the encoder learns contextual features and the decoder takes object queries to generate object proposals. This drastically changes the way object detection is viewed, and inspires several later works on other tasks, such as instance segmentation [12], visual grounding [11], multi-object tracking [53] and HOI detection [16]. HOI detection is most similar to our task, SGG, in that it localizes and recognizes the relationships of each human-object pair. However, there are inherent differences between these two tasks. The HOI task does not need to deal with the $\mathcal{O}(\mathcal{E} \times \mathcal{E})$ space since the subject of each interaction tuple is always the human in the scene. Hence, most of the HOI models cannot be directly transferred to tackle the complexity of the SGG task.

7   Conclusions

Scene graph generation (SGG) deals with two different distributions, namely entities and predicates. Most methods rely on detecting all entities, followed by combining pairs of entites. Unlike such two-stage methods, we propose an end-to-end trainable framework for SGG using a Transformer architecture which decouples these two distributions effectively with conditional queries (TraCQ), leading to a small model size and an efficient inference mechanism. TraCQ significantly outperforms existing single-stage methods, even beating the performance of many state-of-the-art two-stage methods on Visual Genome benchmark.

8   Societal Impacts

SGG models have wide applicability, e.g. caption generation [48, 47], visual question answering [13]. The model itself is harmless and helpful for providing a compact description of the scene. However, there may be some privacy concerns when the model is utilized for monitoring people and their interactions. Note that no explicit recognition is involved in this framework.

9   Limitations

In this paper, we focus on developing a single-stage detector for visual relations. We extensively study different formulations of SGG models with different degrees of entanglement between the predicate and entity detection task. However, we didn't deliberately aimed at addressing the long-tail nature of the two distributions in this work. The unbiased training techniques like resampling or reweighting can be considered in the future work.

Acknowledgments

References

[1] Sherif Abdelkarim, Aniket Agarwal, Panos Achlioptas, Jun Chen, Jiaji Huang, Boyang Li, Kenneth Church, and Mohamed Elhoseiny. Exploring long tail visual relationship recognition with large vocabulary. In *Proceedings of the IEEE/CVF International Conference on Computer Vision*, pages 15921–15930, 2021.

[2] Jimmy Lei Ba, Jamie Ryan Kiros, and Geoffrey E. Hinton. Layer normalization, 2016.

[3] Nicolas Carion, Francisco Massa, Gabriel Synnaeve, Nicolas Usunier, Alexander Kirillov, and Sergey Zagoruyko. End-to-end object detection with transformers. In *Computer Vision – ECCV 2020: 16th European Conference, Glasgow, UK, August 23–28, 2020, Proceedings, Part I*, page 213–229, Berlin, Heidelberg, 2020. Springer-Verlag.

[4] Tianshui Chen, Weihao Yu, Riquan Chen, and Liang Lin. Knowledge-embedded routing network for scene graph generation. In *Conference on Computer Vision and Pattern Recognition*, 2019.

[5] Yuren Cong, Michael Ying Yang, and Bodo Rosenhahn. Reltr: Relation transformer for scene graph generation, 2022.

[6] Alakh Desai, Tz-Ying Wu, Subarna Tripathi, and Nuno Vasconcelos. Learning of visual relations: The devil is in the tails, 2021.

[7] Ross Girshick, Jeff Donahue, Trevor Darrell, and Jitendra Malik. Rich feature hierarchies for accurate object detection and semantic segmentation, 2013.

[8] Nikolaos Gkanatsios, Vassilis Pitsikalis, Petros Koutras, and Petros Maragos. Attention-translation-relation network for scalable scene graph generation. In *Proceedings of the IEEE/CVF International Conference on Computer Vision Workshops*, pages 0–0, 2019.

[9] Jiuxiang Gu, Handong Zhao, Zhe Lin, Sheng Li, Jianfei Cai, and Mingyang Ling. Scene graph generation with external knowledge and image reconstruction. In *Proceedings of the IEEE/CVF conference on computer vision and pattern recognition*, pages 1969–1978, 2019.

[10] Kaiming He, Xiangyu Zhang, Shaoqing Ren, and Jian Sun. Deep residual learning for image recognition. In *IEEE Conference on Computer Vision and Pattern Recognition (CVPR)*, 2016.

[11] Chih-Hui Ho, Srikar Appalaraju, Bhavan Jasani, R Manmatha, and Nuno Vasconcelos. Yoro-lightweight end to end visual grounding. In *ECCV 2022 Workshop on International Challenge on Compositional and Multimodal Perception*, 2022.

[12] Jie Hu, Liujuan Cao, Yao Lu, ShengChuan Zhang, Yan Wang, Ke Li, Feiyue Huang, Ling Shao, and Rongrong Ji. Istr: End-to-end instance segmentation with transformers. *arXiv preprint arXiv:2105.00637*, 2021.

[13] Drew A. Hudson and Christopher D. Manning. GQA: A new dataset for real-world visual reasoning and compositional question answering. In *The IEEE Conference on Computer Vision and Pattern Recognition (CVPR)*, June 2019.

[14] J. Johnson, R. Krishna, M. Stark, L. Li, D. A. Shamma, M. S. Bernstein, and L. Fei-Fei. Image retrieval using scene graphs. In *2015 IEEE Conference on Computer Vision and Pattern Recognition (CVPR)*, volume 00, pages 3668–3678, June 2015.

[15] Justin Johnson, Agrim Gupta, and Li Fei-Fei. Image generation from scene graphs. In *Proceedings of the IEEE Conference on Computer Vision and Pattern Recognition (CVPR)*, June 2018.

[16] Bumsoo Kim, Junhyun Lee, Jaewoo Kang, Eun-Sol Kim, and Hyunwoo J. Kim. Hotr: End-to-end human-object interaction detection with transformers. In *CVPR*. IEEE, 2021.

[17] Rajat Koner, Suprosanna Shit, and Volker Tresp. Relation transformer network. *arXiv preprint arXiv:2004.06193*, 2020.

[18] Ranjay Krishna, Yuke Zhu, Oliver Groth, Justin Johnson, Kenji Hata, Joshua Kravitz, Stephanie Chen, Yannis Kalantidis, Li-Jia Li, David A. Shamma, Michael S. Bernstein, and Fei-Fei Li. Visual genome: Connecting language and vision using crowdsourced dense image annotations. *CoRR*, abs/1602.07332, 2016.

[19] Harold W. Kuhn. The hungarian method for the assignment problem. In *50 Years of Integer Programming*, 2010.

[20] Rongjie Li, Songyang Zhang, and Xuming He. Sgtr: End-to-end scene graph generation with transformer, 2021.

[21] Rongjie Li, Songyang Zhang, Bo Wan, and Xuming He. Bipartite graph network with adaptive message passing for unbiased scene graph generation. In *CVPR*, 2021.

[22] Yikang Li, Tao Ma, Yeqi Bai, Nan Duan, Sining Wei, and Xiaogang Wang. Pastegan: A semi-parametric method to generate image from scene graph. In *Advances in Neural Information Processing Systems 32: Annual Conference on Neural Information Processing Systems 2019, NeurIPS 2019, 8-14, December 2019, Vancouver, BC, Canada*, pages 3950–3960, 2019.

[23] Yikang Li, Wanli Ouyang, Bolei Zhou, Jianping Shi, Chao Zhang, and Xiaogang Wang. Factorizable net: an efficient subgraph-based framework for scene graph generation. In *Proceedings of the European Conference on Computer Vision (ECCV)*, pages 335–351, 2018.

[24] Yikang Li, Wanli Ouyang, Bolei Zhou, Kun Wang, and Xiaogang Wang. Scene graph generation from objects, phrases and region captions. In *Proceedings of the IEEE international conference on computer vision*, pages 1261–1270, 2017.

[25] Xin Lin, Changxing Ding, Jinquan Zeng, and Dacheng Tao. Gps-net: Graph property sensing network for scene graph generation, 2020.

[26] Hengyue Liu, Ning Yan, Masood Mortazavi, and Bir Bhanu. Fully convolutional scene graph generation. In *Proceedings of the IEEE/CVF Conference on Computer Vision and Pattern Recognition (CVPR)*, pages 11546–11556, June 2021.

[27] Ilya Loshchilov and Frank Hutter. Decoupled weight decay regularization, 2017.

[28] Yichao Lu, Himanshu Rai, Jason Chang, Boris Knyazev, Guangwei Yu, Shashank Shekhar, Graham W Taylor, and Maksims Volkovs. Context-aware scene graph generation with seq2seq transformers. In *Proceedings of the IEEE/CVF International Conference on Computer Vision*, pages 15931–15941, 2021.

[29] Kien Nguyen, Subarna Tripathi, Bang Du, Tanaya Guha, and Truong Q. Nguyen. In defense of scene graphs for image captioning. In *Proceedings of the IEEE/CVF International Conference on Computer Vision (ICCV)*, pages 1407–1416, October 2021.

[30] Tianwen Qian, Jingjing Chen, Shaoxiang Chen, Bo Wu, and Yu-Gang Jiang. Scene graph refinement network for visual question answering. *IEEE Transactions on Multimedia*, pages 1–1, 2022.

[31] Shaoqing Ren, Kaiming He, Ross Girshick, and Jian Sun. Faster r-cnn: Towards real-time object detection with region proposal networks. In C. Cortes, N. Lawrence, D. Lee, M. Sugiyama, and R. Garnett, editors, *Advances in Neural Information Processing Systems*, volume 28, pages 91–99. Curran Associates, Inc., 2015.

[32] Hamid Rezatofighi, Nathan Tsoi, JunYoung Gwak, Amir Sadeghian, Ian Reid, and Silvio Savarese. Generalized intersection over union: A metric and a loss for bounding box regression, 2019.

[33] Suprosanna Shit, Rajat Koner, Bastian Wittmann, Johannes Paetzold, Ivan Ezhov, Hongwei Li, Jiazhen Pan, Sahand Sharifzadeh, Georgios Kaissis, Volker Tresp, and Bjoern Menze. Relationformer: A unified framework for image-to-graph generation, 2022.

[34] Kaihua Tang, Yulei Niu, Jianqiang Huang, Jiaxin Shi, and Hanwang Zhang. Unbiased scene graph generation from biased training. In *2020 IEEE/CVF Conference on Computer Vision and Pattern Recognition, CVPR 2020, Seattle, WA, USA, June 13-19, 2020*, pages 3713–3722. IEEE, 2020.

[35] Kaihua Tang, Hanwang Zhang, Baoyuan Wu, Wenhan Luo, and Wei Liu. Learning to compose dynamic tree structures for visual contexts. In *The IEEE Conference on Computer Vision and Pattern Recognition (CVPR)*, June 2019.

[36] Hung-Yu Tseng, Hsin ying Lee, Lu Jiang, Ming-Hsuan Yang, and Weilong Yang. RetrieveGAN: Image synthesis via differentiable patch retrieval. In *ECCV*, 2020.

[37] Ashish Vaswani, Noam Shazeer, Niki Parmar, Jakob Uszkoreit, Llion Jones, Aidan N Gomez, Ł ukasz Kaiser, and Illia Polosukhin. Attention is all you need. In I. Guyon, U. Von Luxburg, S. Bengio, H. Wallach, R. Fergus, S. Vishwanathan, and R. Garnett, editors, *Advances in Neural Information Processing Systems*, volume 30. Curran Associates, Inc., 2017.

[38] Sijin Wang, Ruiping Wang, Ziwei Yao, Shiguang Shan, and Xilin Chen. Cross-modal scene graph matching for relationship-aware image-text retrieval. In *IEEE Winter Conference on Applications of Computer Vision, WACV 2020, Snowmass Village, CO, USA, March 1-5, 2020*, pages 1497–1506. IEEE, 2020.

[39] Tao Wang, Li Yuan, Yunpeng Chen, Jiashi Feng, and Shuicheng Yan. Pnp-detr: Towards efficient visual analysis with transformers. In *Proceedings of the IEEE/CVF International Conference on Computer Vision*, pages 4661–4670, 2021.

[40] Tzu-Jui Julius Wang, Selen Pehlivan, and Jorma Laaksonen. Tackling the unannotated: Scene graph generation with bias-reduced models. *arXiv preprint arXiv:2008.07832*, 2020.

[41] Wenbin Wang, Ruiping Wang, Shiguang Shan, and Xilin Chen. Exploring context and visual pattern of relationship for scene graph generation. In *Proceedings of the IEEE/CVF Conference on Computer Vision and Pattern Recognition*, pages 8188–8197, 2019.

[42] Sanghyun Woo, Dahun Kim, Donghyeon Cho, and In So Kweon. Linknet: Relational embedding for scene graph. *Advances in Neural Information Processing Systems*, 31, 2018.

[43] Danfei Xu, Yuke Zhu, Christopher Choy, and Li Fei-Fei. Scene graph generation by iterative message passing. In *Computer Vision and Pattern Recognition (CVPR)*, 2017.

[44] Shaotian Yan, Chen Shen, Zhongming Jin, Jianqiang Huang, Rongxin Jiang, Yaowu Chen, and Xian-Sheng Hua. PCPL: predicate-correlation perception learning for unbiased scene graph generation. In *MM '20: The 28th ACM International Conference on Multimedia, Virtual Event / Seattle, WA, USA, October 12-16, 2020*, pages 265–273, 2020.

[45] Jianwei Yang, Jiasen Lu, Stefan Lee, Dhruv Batra, and Devi Parikh. Graph r-cnn for scene graph generation, 2018.

[46] Jianwei Yang, Jiasen Lu, Stefan Lee, Dhruv Batra, and Devi Parikh. Graph r-cnn for scene graph generation. In *Proceedings of the European conference on computer vision (ECCV)*, pages 670–685, 2018.

[47] Xu Yang, Kaihua Tang, Hanwang Zhang, and Jianfei Cai. Auto-encoding scene graphs for image captioning. In *The IEEE Conference on Computer Vision and Pattern Recognition (CVPR)*, June 2019.

[48] Ting Yao, Yingwei Pan, Yehao Li, and Tao Mei. Exploring visual relationship for image captioning. In *The European Conference on Computer Vision (ECCV)*, September 2018.

[49] Guojun Yin, Lu Sheng, Bin Liu, Nenghai Yu, Xiaogang Wang, Jing Shao, and Chen Change Loy. Zoom-net: Mining deep feature interactions for visual relationship recognition. In *Proceedings of the European Conference on Computer Vision (ECCV)*, pages 322–338, 2018.

[50] Ruichi Yu, Ang Li, Vlad I Morariu, and Larry S Davis. Visual relationship detection with internal and external linguistic knowledge distillation. In *Proceedings of the IEEE international conference on computer vision*, pages 1974–1982, 2017.

[51] Alireza Zareian, Svebor Karaman, and Shih-Fu Chang. Bridging knowledge graphs to generate scene graphs. In *European Conference on Computer Vision*, pages 606–623. Springer, 2020.

[52] Rowan Zellers, Mark Yatskar, Sam Thomson, and Yejin Choi. Neural motifs: Scene graph parsing with global context. *CoRR*, abs/1711.06640, 2017.

[53] Fangao Zeng, Bin Dong, Yuang Zhang, Tiancai Wang, Xiangyu Zhang, and Yichen Wei. Motr: End-to-end multiple-object tracking with transformer. *arXiv preprint arXiv:2105.03247*, 2021.

[54] Hanwang Zhang, Zawlin Kyaw, Shih-Fu Chang, and Tat-Seng Chua. Visual translation embedding network for visual relation detection. In *Proceedings of the IEEE conference on computer vision and pattern recognition*, pages 5532–5540, 2017.

Checklist

1. For all authors...
   - (a) Do the main claims made in the abstract and introduction accurately reflect the paper's contributions and scope? [Yes]
   - (b) Did you describe the limitations of your work? [Yes]
   - (c) Did you discuss any potential negative societal impacts of your work? [Yes]
   - (d) Have you read the ethics review guidelines and ensured that your paper conforms to them? [Yes]
2. If you are including theoretical results...

(a) Did you state the full set of assumptions of all theoretical results? [N/A]

(b) Did you include complete proofs of all theoretical results? [N/A]

3. If you ran experiments...

(a) Did you include the code, data, and instructions needed to reproduce the main experimental results (either in the supplemental material or as a URL)? [No] The code will be released.

(b) Did you specify all the training details (e.g., data splits, hyperparameters, how they were chosen)? [Yes]

(c) Did you report error bars (e.g., with respect to the random seed after running experiments multiple times)? [No]

(d) Did you include the total amount of compute and the type of resources used (e.g., type of GPUs, internal cluster, or cloud provider)? [Yes]

4. If you are using existing assets (e.g., code, data, models) or curating/releasing new assets...

(a) If your work uses existing assets, did you cite the creators? [Yes]

(b) Did you mention the license of the assets? [N/A]

(c) Did you include any new assets either in the supplemental material or as a URL? [No]

(d) Did you discuss whether and how consent was obtained from people whose data you're using/curating? [N/A]

(e) Did you discuss whether the data you are using/curating contains personally identifiable information or offensive content? [N/A]

5. If you used crowdsourcing or conducted research with human subjects...

(a) Did you include the full text of instructions given to participants and screenshots, if applicable? [N/A]

(b) Did you describe any potential participant risks, with links to Institutional Review Board (IRB) approvals, if applicable? [N/A]

(c) Did you include the estimated hourly wage paid to participants and the total amount spent on participant compensation? [N/A]